JACS
JOURNAL OF THE AMERICAN CHEMICAL SOCIETY

Communication

pubs.acs.org/JACS

Exploiting Specific Interactions toward Next-Generation Polymeric Drug Transporters

Sebastian Wieczorek,[#] Eberhard Krause,[‖] Steffen Hackbarth,[×] Beate Röder,[×] Anna K. H. Hirsch,[§] and Hans G. Börner*[,#]

[#]Laboratory for Organic Synthesis of Functional Systems, Department of Chemistry, Humboldt-Universität zu Berlin, Brook-Taylor-Strasse 2, D-12489 Berlin, Germany

[‖]Leibniz-Institut für Molekulare Pharmakologie (FMP), Robert-Rössle-Strasse 10, D-13125 Berlin, Germany

[×]Department of Physics, Humboldt-Universität zu Berlin, Newton Strasse 15, D-12489 Berlin, Germany

[§]Stratingh Institute for Chemistry, University of Groningen, Nijenborgh 7, NL-9747 AG Groningen, The Netherlands

Supporting Information

ABSTRACT: A generic method describes advanced tailoring of polymer drug carriers based on polymer-*block*-peptides. Combinatorial means are used to select suitable peptide segments to specifically complex small-molecule drugs. The resulting specific drug formulation agents render insoluble drugs water-soluble and enable precise adjustment of drug-release profiles beyond established block-copolymer carriers. While proof of principle is shown on chlorin as a partially approved drug for photodynamic cancer therapy, the concept is universal and applies to a broad spectrum of difficult drugs.

A major difficulty in pharmacological drug development results from poor water solubility of the lead compound,[1] from which low bioavailability, uncontrolled drug partitioning, and severe adverse effects can result.[2] Strategies to overcome these properties of problematic drugs include combinatorial screening of structurally derived compound libraries, consecutive structure adaption cycles, and knowledge-based optimization.[3] However, structural modification of highly potent entities might jeopardize drug activity.[4] Drug-formulation strategies offer an alternative approach.[5] Among others, synthetic polymers proved their potential by enabling stealth delivery, active drug release, improved biobarrier translocation, or passive targeting.[2,6] Polymers have become extensively used as solubilization agents,[7] but compound-specific interactions as occurring in biological protein-based transporters are difficult to realize with established block copolymers.[8] Supramolecular host/guest complexes such as core-designed dendrimers or macrocycles have been employed to bind drugs specifically via a set of combined soft interactions,[9] but the synthetic effort required for adaptation limits the development of generic transporter platforms. Over the past decade, peptide/polymer conjugates have shown high potential for materials science and biomedical applications.[10] New possibilities arise from full sequence control of the peptide segment, offering precisely adjustable interaction capabilities as one key parameter to realize specific drug solubilizers.[11]

Tetrapyrroles constitute a highly promising class of drugs for photodynamic cancer therapy (PDT).[12] Among them, *m*-tetra(hydroxyphenyl)chlorin (*m*-THPC, Figure 1)[13] shows

Figure 1. *m*-Tetra(hydroxyphenyl)chlorin photosensitizer (left) and sequences of the complementary conjugate transporters (right).

effective photosensitization of singlet oxygen ($^1O_2$) and was partially approved for use against head and neck squamous cell carcinoma.[14] Shape anisotropy and electronic π-interactions of *m*-THPC drive intermolecular aggregation and limit its water solubility. Despite it being administered as a multicomponent formulation, some reports describe the occurrence of uncontrolled drug partitioning in lipophilic membranes and/or slow solubilization by plasma proteins, namely human serum albumin (HSA).[14] Common formulation agents, e.g., Pluronic,[15] do not show significant improvements, as those micellar carriers solubilize *m*-THPC well but effective release of the active compound is often too slow, making patients suffer from light sensitivity over days.[14] Thus, tailor-made solubilizers are required that improve the solubility of *m*-THPC and allow for adjustment of drug-release kinetics. Recently, we showed that peptide/polymer conjugates afford sequence-specific solubilization of inhibitors of the kinase IspE,[16] an antimalarial target. The empirical design strategy used, however, might have overlooked most effective host peptide sequences.

Figure 2. Schematic illustration of the screening and synthesis procedure to identify peptide sequences for specific solubilization of *m*-THPC.

Received: December 6, 2012
Published: January 11, 2013

dx.doi.org/10.1021/ja311895z | *J. Am. Chem. Soc.* 2013, 135, 1711−1714

Here we study tailor-made solubilizers to specifically host polar water-insoluble photosensitizers, overcoming the solubility problem of *m*-THPC in water. Combinatorial means are used to select the most suitable peptide sequences in a straightforward manner. A one-bead/one-component peptide library was synthesized by solid-phase supported split-and-mix procedures (Figure 2).[17] Looking at the structure of *m*-THPC, interactions with aromatic, anionic, hydrophobic, and H-bonding groups can be anticipated. Thus, Gly, Leu, Ser, Phe, Glu, Gln, and Lys were incorporated at each amino acid position in a set of 7mer peptides, giving 8.2×10^5 sequence variations. A C-terminal Gly-Gly-Met linker connected the peptides to the support, allowing both deprotection of supported peptides by TFA and peptide release for analytical purposes by cyanogen bromide.

The fully deprotected peptide library was incubated with a suspension of *m*-THPC in water and EtOH. Partitioning of the photosensitizer in the library was followed by fluorescence microscopy, taking advantage of the fluorescence properties of *m*-THPC (Figures 2 and S2). Positive hits, based on fluorescent single polymer beads, were separated to identify peptide sequences with high affinity to complex *m*-THPC. Single-bead peptide sequencing was done by MALDI-ToF-MS/MS spectrometry. MS analysis of 41 highly fluorescent beads gave a set of amino acid sequences (Table S1). Sequence evaluation identifies high propensities to find several Phe residues enclosing a central amino acid, which could be hydrophobic Leu, negatively charged Glu, or a combination of Glu-Gln. The aromatic Phe segments are often flanked by polar amino acids such as Ser or Gln. These findings were merged into three peptide sequences (**I**–**III**) that should provide high affinity to bind *m*-THPC in water. To study the properties of the selected sequences, peptide-*block*-poly(ethylene oxide) (peptide-PEO) conjugates (**P I**–**P III**, Figure 1) were synthesized by SPPS via an inverse conjugation strategy.[18] Conceptually, the peptide segments are responsible for specific drug binding, and the PEO blocks provide shielding as well as water solubility. A PEO block of $M_n = 3200$ was chosen, giving bioconjugates of <5 kDa that can be cleared from the biosystem by renal ultrafiltration after use.

Solubilization experiments on *m*-THPC with each of the bioconjugates suggest that all three peptides can effectively solubilize *m*-THPC in water; however, the peptide sequences crucially affect the solubilization capacities (Figure 3). A freeze-dry procedure was followed, enabling rapid determination of maximum loading of the bioconjugate carriers with *m*-THPC. Aqueous solutions of the various carriers were added to ethanolic *m*-THPC solutions. The mixtures obtained were lyophilized, redissolved in pure water, and nonsolubilized *m*-THPC was removed by centrifugation. UV/vis spectroscopy of the supernatants showed typical absorption spectra of *m*-THPC, whereas controls with either pure water or PEO showed no evidence of *m*-THPC (Figure 3).

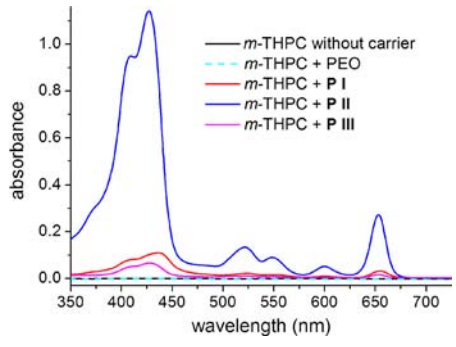

Figure 3. Absorption spectra of *m*-THPC solubilization experiments with peptide-PEO conjugates and controls. Conditions: [conjugates] = 15 μM in water, rt, pH 7.

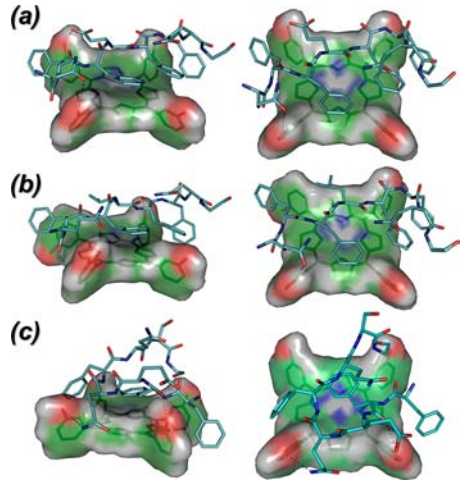

Figure 4. Idealized docking of *m*-THPC (shown as van der Waals surface) binding to peptide host sequences (shown as sticks) in a 1:1 complex: (a) **I**/*m*-THPC, (b) **II**/*m*-THPC, and (c) **III**/*m*-THPC. Modeled with MOLOC; left, side view, and right, top view.

UV/vis spectroscopy allows quantification of the solubilization experiments. The total concentration of solubilized *m*-THPC through each bioconjugate was determined by measuring the molar extinction at 650 nm of the carrier/drug complexes in ethanol. Significant differences were observed, highlighting the importance of the peptide sequence for the solubilization capacities. **P II**, with a central Leu residue, showed the highest payload capacity, 0.31 mmol of drug/mmol of carrier. Counter-intuitively, **P I** and **P III**, both with an apparently suitable negatively charged Glu residue between the Phe segments, were much less effective, at 0.06 and 0.03 mmol of drug/mmol of carrier, respectively.

It is noteworthy that the selected peptides provide, within their order of presented functionalities, intimate information on the requirements for interactions at the molecular level. To understand the sequence dependency of the solubilization, idealized 1:1 complexes of *m*-THPC and peptides **I**–**III** (omitting the PEO moiety) were modeled[19] with the software MOLOC (cf. Figure 4 and SI). Analysis of the non-covalent interactions revealed π-stacking of Phe residues and the aromatic chlorin scaffold as the dominant cargo/transporter interaction for **P I**–**P III**. Furthermore, flanking N- and C-terminal Gln residues (**P I** and **P II**) form H-bonds to the phenolic *m*-THPC substituents. Interestingly, the carboxylate functionality of the central Glu of **P I** interacts not with the amine or imine core of the tetrapyrrole ring, but with the outer hydroxyl groups. For **P III**, it seems more favorable for the central Gln-Glu residues to bend away from the tetrapyrrole ring to interact with hydroxyphenyl rings and surrounding water. Using the docking program LeadIT, the modeled poses were ranked according to their binding free energies as calculated by the HYDE scoring function as implemented in LeadIT. The predicted binding energies correlate with the experimental data found by solubilization studies. While **P I** and **P III** gave a predicted value of −23 kJ/mol, the most effective solubilizer (**P II**) is predicted to have a free energy of binding of −29 kJ/mol. Despite

dx.doi.org/10.1021/ja311895z | *J. Am. Chem. Soc.* 2013, 135, 1711–1714

the interesting insights into binding interactions, the model character of the simulations should be emphasized. The relation of the molecular dimensions makes carrier/drug complex formation with a 1:1 stoichiometry unlikely to occur. However, from the idealized complexes, essential binding motifs are revealed, which certainly will be more likely to occur in the actual drug/carrier complexes.

Besides the solubilization of *m*-THPC, the drug function with respect to PDT is of interest. To examine the activity of solubilized *m*-THPC, initial fluorescence-emission spectra were recorded because the fluorescence properties correlate with the ability to generate $^1O_2$. Interestingly, all peptide-PEO conjugates carry their maximum payload of *m*-THPC, but clear solutions show no or very little fluorescence emission (data not shown). This effect can probably be attributed to intermolecular quenching of *m*-THPC, suggesting the absence of molecularly solubilized sensitizers, and might indicate the presence of, e.g., micellar solubilization. To confirm this, the different cargo/transporter solutions were analyzed by dynamic light scattering (Table S4). All three systems showed aggregate formation. **P I**/*m*-THPC and **P III**/*m*-THPC displayed hydrodynamic radii (R_h) of ∼65 and ∼75 nm, respectively, whereas **P II**/*m*-THPC yielded a broad distribution with R_h centered at ∼165 nm. Pure bioconjugate solutions of **P I** and **P III** without *m*-THPC showed no detectable aggregates. The more hydrophobic sequence of **P II** induced micelle formation already in the absence of *m*-THPC with $R_h \approx 40$ nm. With respect to the generality of the presented approach, the PEO/peptide block length ratio might be a way to tune cargo capacity (payload) and effectiveness of drug shielding as well as type and size of formed aggregates. The influence of PEO length on drug cargo properties will be reported elsewhere. Taking into account the requirements for transport of photosensitizers for PDT, micellar solubilization would be highly beneficial. The sensitizer is inactivated during transport until release from the carrier, thereby diminishing undesired toxicity and increasing shelf life. This inactive transport state was confirmed by the absence of $^1O_2$ luminescence for each of the solubilized *m*-THPC systems in water (data not shown).

This finding puts into focus the release profile of the drug from the silent transport state to an active state. Photosensitizers for PDT might be intravenously administered, followed by systemic distribution through the blood to reach their target tissues. From the literature, it is accepted that hydrophobic drugs in the blood transfer rapidly to serum albumin transporter proteins or other plasma proteins. Thus, it is important to study drug cross-solubilization (release from the bioconjugate carrier) toward serum albumin. Dilute solutions of *m*-THPC-saturated bioconjugates were exposed to an excess of bovine serum albumin (BSA), used as a model for HSA. The release kinetics can be conveniently followed by the development of *m*-THPC fluorescence (Figure 5). Intermolecular quenching of sensitizer molecules in the bioconjugate aggregates diminishes during cross-transfer to BSA. **P III** and **P I** show effective release of *m*-THPC cargo, reaching 50% of the sensitizer in an active state after 3 and 5 h, respectively, as well as about 90% activity after ∼13 and 21 h, respectively. Fluorescence intensity increases noticeably faster for cargo release from **P II**, reaching 50% activity after ∼2 h. Interestingly, the release slows down significantly after 2 h. Combining burst-and-retard release might even be advantageous for drug administration. These results highlight strong sequence dependency of the release kinetics. A single-residue exchange (Leu4→Glu4) in the peptide sequence of the transporter **P II** and **P I** distinctly alters the release profile. This provides a potent handle to tailor release kinetics accurately for polymer-based drug transporters, depending on the demands.

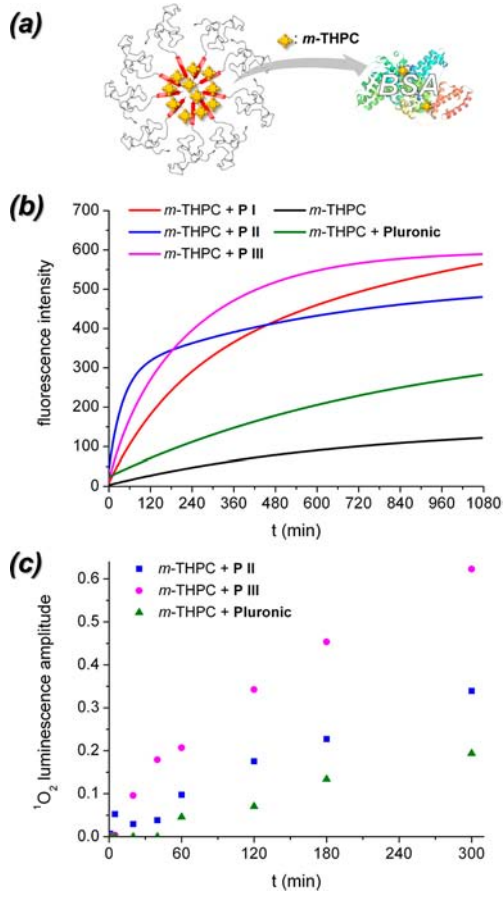

Figure 5. (a) Schematic illustration of peptide-PEO aggregates loaded with *m*-THPC and cross-diffusion to BSA (PDB 3V03). (b) Fluorescence increase of solutions of *m*-THPC/solubilizer complexes in the presence of BSA. (c) Development of $^1O_2$ production. Conditions: (b) λ_{ex} = 417 nm, λ_{em} = 653 nm, [BSA] = 50 μM, [*m*-THPC] = 1 μM; (c) λ_{ex} = 425 nm, λ_{em} = 1270 nm, [BSA] = 100 μM, [*m*-THPC] = 2 μm. Signal amplitudes are given relative to the values after 100 h.

The tailor-made specific solubilizers were also compared to Pluronic (F68) drug formulation agent as a relevant control.[15] F68 shows 5 times higher loading capacity for *m*-THPC, outcompeting **P II**, but with an unfavorable release of the sensitizer (Figure 5). *m*-THPC activation from F68 aggregates occurs slowly and reaches ∼40% activity after 18 h. This reflects a common drawback of polymeric carrier systems: because they bind their cargo through unspecific hydrophobic interactions, the drug release is not easily tunable. Slow release profiles, as observed for release from F68 carriers as well as during direct solubilization of *m*-THPC with BSA (Figure 5), are considered to be most problematic for PDT. Slow activation kinetics might cause prolonged light sensitivity for time periods of up to 7 days, which could potentially lead to blindness in the worst case.[12]

While fluorescence is an indicator for *m*-THPC activity, ultimate proof of drug function requires measuring $^1O_2$-production rates. A time-dependent measurement of $^1O_2$ luminescence was performed (Figure 5), enabling to follow the transition from the silent transport form of *m*-THPC hosted in

dx.doi.org/10.1021/ja311895z | J. Am. Chem. Soc. 2013, 135, 1711−1714

bioconjugate carriers toward the pharmaceutically active drug cross-solubilized in albumins. Quantitative determination of the $^1O_2$ generated by irradiation with LED light of around 425 nm confirms the strong and sensitive sequence dependency of the sensitizer-activation kinetics. The development of $^1O_2$ production correlates well with the fluorescence data. Slight differences observed can be explained by the fact that $^1O_2$ production depends on excitability and O_2 accessibility. After 100 h, all transport systems reach practically the same $^1O_2$ quantum efficiency. The development depends significantly on the carrier. Pluronic F68 has the slowest activation kinetics, reaching ∼20% *m*-THPC activity after 5 h, at which point the **P III** system already has ∼60% sensitizer activated. The **P II** solubilizers combine high loading capacity with acceptable $^1O_2$-production rates and thus represent an excellent starting point to develop a next-generation drug transporter for *m*-THPC. Detailed analysis of the fluorescence anisotropy provides insight into the trans-solubilization process that probably occurs via a collision mechanism between BSA and *m*-THPC-loaded peptide-PEO aggregates. More-detailed studies are required to elucidate the exact processes.

In conclusion, a fluorescence-based screening method was established to assist the design of peptide-*block*-poly(ethylene oxide) copolymers to specifically host the photosensitizer *m*-tetra(hydroxyphenyl)chlorin. Solubilization capacity (maximum payload of *m*-THPC in the bioconjugates) and release kinetics from the transport system proved to depend strongly on the peptide sequence of the peptide-PEO conjugates. Most favorable for a photosensitizer transport system, an effective solubilization process led to micellar solubilized drugs, which exhibit a silent transport state with very low or no activity, as indicated by direct singlet-oxygen-generation measurements. Depending on the peptide-binding domain, the transporters release the cargo to serum albumin protein. Tunable release profiles can be programmed in the peptide segment, which is an improvement over established polymeric solubilizers. Solubility, dispersibility, and compatibility of small functional compounds appear to be problematic not only in biomedicine but also in fields ranging from demixing of UV stabilizers in polymers to incompatibility of additives in engine lubricants to surface remodulation in coatings. It is foreseeable that specific hosting of active compounds can be of advantage beyond drug transporters.

■ ASSOCIATED CONTENT

Supporting Information

Experimental procedures and analytical data. This material is available free of charge via the Internet at http://pubs.acs.org.

■ AUTHOR INFORMATION

Corresponding Author

h.boerner@hu-berlin.de

Notes

The authors declare no competing financial interest.

■ ACKNOWLEDGMENTS

We acknowledge M. Senge (Trinity College Dublin) for providing *m*-THPC, H. Stephanowitz (FMP) for MS, K. Linkert (HU) for SPPS, H. Schlaad, A. Völkel (MPIKG) for DLS, T. Masini (University of Groningen) for modeling and C. Arenz, S. Neubacher (HU) for helpful discussion. Funding was granted by the European Research Council under the European Union's 7th Framework Program (FP07-13)/ERC Starting grant "Specifically Interacting Polymer−SIP" (ERC 305064) (H.G.B.) and The Netherlands Organization for Scientific Research (NWO-CW, VENI grant) (A.K.H.H.).

■ REFERENCES

(1) Lipinski, C. A.; Lombardo, F.; Dominy, B. W.; Feeney, P. J. *Adv. Drug Delivery Rev.* **2001**, *46*, 3. Singh, A.; Worku, Z. A.; Van den Mooter, G. *Exp. Opin. Drug Delivery* **2011**, *8*, 1361. Kennedy, T. *Drug Discov. Today* **1997**, *2*, 436.

(2) Duncan, R. *Nat. Rev. Drug Discov.* **2003**, *2*, 347.

(3) Guido, R. V. C.; Oliva, G.; Andricopulo, A. D. *Comb. Chem. High Throughput Screen* **2011**, *14*, 830. Hajduk, P. J.; Greer, J. *Nat. Rev. Drug Discov.* **2007**, *6*, 211. Andricopulo, A. D.; Salum, L. B.; Abraham, D. J. *Curr. Top. Med. Chem.* **2009**, *9*, 771.

(4) Manly, C. J.; Chandrasekhar, J.; Ochterski, J. W.; Hammer, J. D.; Warfield, B. B. *Drug Discov. Today* **2008**, *13*, 99.

(5) Williams, R. O., Watts, A. B., Miller, D. A., Eds. Formulating Poorly Water Soluble Drugs. In *AAPS Advances in the Pharmaceutical Sciences Series*, Vol. 3; Springer: Berlin, 2012; p 658. Torchilin, V. P. *Exp. Opin. Ther. Pat.* **2005**, *15*, 63. Kataoka, K.; Harada, A.; Nagasaki, Y. *Adv. Drug Delivery Rev.* **2001**, *47*, 113.

(6) Ferrari, M. *Nat. Rev. Cancer* **2005**, *5*, 161. Fleige, E.; Quadir, M. A.; Haag, R. *Adv. Drug Delivery Rev.* **2012**, *64*, 866. Meyer, M.; Philipp, A.; Oskuee, R.; Schmidt, C.; Wagner, E. *J. Am. Chem. Soc.* **2008**, *130*, 3272.

(7) Fox, M. E.; Szoka, F. C.; Frechet, J. M. J. *Acc. Chem. Res.* **2009**, *42*, 1141. Allen, T. M.; Cullis, P. R. *Science* **2004**, *303*, 1818. Bae, Y.; Kataoka, K. *Adv. Drug Delivery Rev.* **2009**, *61*, 768. Kabanov, A. V.; Vinogradov, S. V. *Angew. Chem., Int. Ed.* **2009**, *48*, 5418. Knop, K.; Hoogenboom, R.; Fischer, D.; Schubert, U. S. *Angew. Chem., Int. Ed.* **2010**, *49*, 6288. Deming, T. J. *Prog. Polym. Sci.* **2007**, *32*, 858.

(8) Schneider, H. J. *Angew. Chem., Int. Ed.* **2009**, *48*, 3924. Torchilin, V. P. *Pharm. Res.* **2007**, *24*, 1.

(9) Lee, C. C.; MacKay, J. A.; Frechet, J. M. J.; Szoka, F. C. *Nat. Biotechnol.* **2005**, *23*, 1517. Menjoge, A. R.; Kannan, R. M.; Tomalia, D. A. *Drug Discov. Today* **2010**, *15*, 171. Hecht, S.; Frechet, J. M. J. *Angew. Chem., Int. Ed.* **2001**, *40*, 74. Saleh, N. i.; Koner, A. L.; Nau, W. M. *Angew. Chem., Int. Ed.* **2008**, *47*, 5398. Gebauer, M.; Skerra, A. *Curr. Opin. Chem. Biol.* **2009**, *13*, 245.

(10) Elsabahy, M.; Wooley, K. L. *Chem. Soc. Rev.* **2012**, *41*, 2545. Schwemmer, T.; Baumgartner, J.; Faivre, D.; Börner, H. G. *J. Am. Chem. Soc.* **2012**, *134*, 2385. Kolodziej, C. M.; Kim, S. H.; Broyer, R. M.; Saxer, S. S.; Decker, C. G.; Maynard, H. D. *J. Am. Chem. Soc.* **2012**, *134*, 247. Wilke, P.; Börner, H. G. *ACS Macro Lett.* **2012**, *1*, 871−875. Matmour, R.; De Cat, I.; George, S. J.; Adriaens, W.; Leclere, P.; Bomans, P. H. H.; Sommerdijk, N.; Gielen, J. C.; Christianen, P. C. M.; Heldens, J. T.; van Hest, J. C. M.; Lowik, D.; De Feyter, S.; Meijer, E. W.; Schenning, A. *J. Am. Chem. Soc.* **2008**, *130*, 14576. Hartmann, L.; Börner, H. G. *Adv. Mater.* **2009**, *21*, 3425. Kühnle, R. I.; Börner, H. G. *Angew. Chem., Int. Ed.* **2011**, *50*, 4499. Hentschel, J.; Bleek, K.; Ernst, O.; Lutz, J.-F.; Börner, H. G. *Macromolecules* **2008**, *41*, 1073.

(11) Börner, H. G. *Macromol. Rapid Commun.* **2011**, *32*, 115.

(12) O'Connor, A. E.; Gallagher, W. M.; Byrne, A. T. *Photochem. Photobiol.* **2009**, *85*, 1053.

(13) Wiehe, A.; Simonenko, E. J.; Senge, M. O.; Röder, B. *J. Pept. Res.* **2001**, *5*, 758.

(14) Senge, M. O. *Photodiag. Photodyn. Ther.* **2012**, *9*, 170.

(15) Batrakova, E. V.; Kabanov, A. V. *J. Controlled Rel.* **2008**, *130*, 98.

(16) Hirsch, A. K. H.; Diederich, F.; Antonietti, M.; Börner, H. G. *Soft Matter* **2010**, *6*, 88.

(17) Lam, K. S.; Salmon, S. E.; Hersh, E. M.; Hruby, V. J.; Kazmierski, W. M.; Knapp, R. J. *Nature* **1991**, *354*, 82. Wennemers, H. *Comb. Chem. High Throughput Screen* **2001**, *4*, 273.

(18) Lutz, J.-F.; Börner, H. G. *Prog. Polym. Sci.* **2008**, *33*, 1.

(19) Gerber, P. R.; Müller, K. *J. Comput.-Aided Mol. Des.* **1995**, *9*, 251. Schneider, N.; Reulecke, I.; Lange, G.; Albrecht, J.; Klein, R.; Rarey, M. *ChemMedChem* **2008**, *3*, 885. Hindle, S.; Lange, G.; Klein, R.; Albrecht, J.; Briem, H.; Beyer, K.; Claußen, H.; Gastreich, H.; Lemmen, C.; Rarey, M. *J. Comput.-Aided Mol. Des.* **2012**, *23*, 869.